0–40 GHz GaAs MESFET Distributed Baseband Amplifier IC's for High-Speed Optical Transmission

Shunji Kimura, *Member, IEEE*, and Yuhki Imai, *Member, IEEE*

***Abstract*— We describe distributed amplifiers built using advanced circuit design techniques to improve gain and noise performance at low frequencies. Using these techniques, we have developed an amplifier IC with a 0–36 GHz bandwidth and a noise figure of 4 dB at low frequencies. This frequency range starting from 0 Hz makes it possible to use the IC as a baseband amplifier for SDH optical transmission systems and this noise figure is about 1 dB better than conventional distributed amplifiers. We also present another amplifier IC built using our loss compensation technique to improve high-frequency performance of the amplifier. This IC has a 0–44-GHz bandwidth, which is the widest among all reported GaAs MESFET baseband amplifiers.**

I. Introduction

A BASEBAND amplifier operating from 0 Hz to several-tens GHz with a low noise figure is required for very high-speed optical transmission systems. The required lower limit frequency of the amplifier is determined by the section length in the bit stream. The transfer section overhead is included in the bit stream every 125 μs, which corresponds to a frequency of 8 kHz. In current systems, we consequently adopted a dc amplifier with the direct-coupling architecture and feed-back configurations shown in Fig. 1 [1]. These kinds of amplifiers have a high and flat gain from 0 Hz but high-frequency performance is limited by the parasitic capacitances of the transistors. Their upper limit frequency is empirically known to achieve only a 30% of the transition frequency (f_T) of the transistors. If we use commercially-available GaAs MESFET's, which have the f_T of 40 GHz, we can achieve only a 12~13-GHz bandwidth with this lumped-circuit design techniques.

On the other hand, the distributed amplifying technique has been widely applied in several-GHz-to-several-tens-GHz-bandwidth amplifiers [2]–[4]. They have artificial input and output lines that are constructed with a series of transmission lines and the parasitic capacitances of the transistors (Fig. 2). These lines have very high cut-off frequencies and cancel out the effects of parasitic capacitances. So, these amplifiers inherently have wideband characteristics. However, with conventional design techniques, gain and noise performance are low at relatively low frequencies. This makes it very difficult to produce a baseband amplifier for optical transmission systems.

This paper describes two innovative techniques for designing the termination circuits of the artificial lines that overcome these problems. A key feature is the use of frequency-dependent drain termination and active gate termination to achieve a 0-Hz-to-millimeter-wave bandwidth with a low noise figure. Moreover, high-frequency performance of the distributed amplifier is also limited due to high artificial-line losses. We adopted our loss compensation technique [5] to achieve over-40-GHz bandwidth with commercially-available GaAs MESFET's.

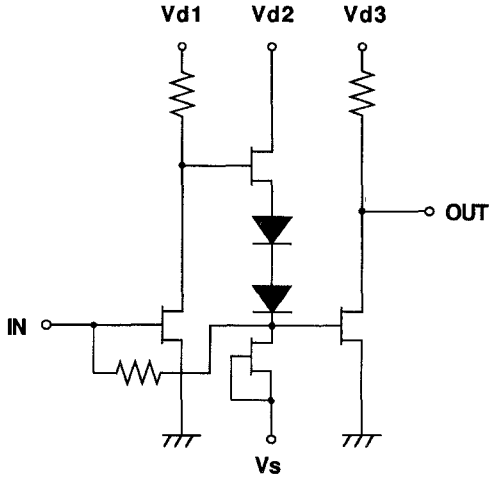

Fig. 1. Schematic circuit of a conventional baseband amplifier.

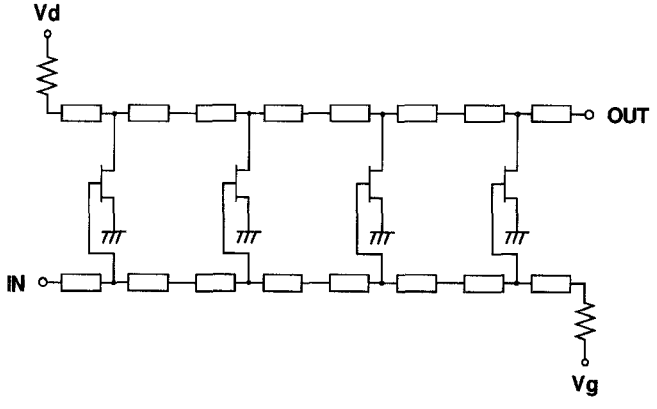

Fig. 2. Schematic circuit of a conventional distributed amplifier.

II. Circuit Design

A schematic circuit of the distributed baseband amplifier with the frequency-dependent drain termination and active gate termination is shown in Fig. 3. We discuss the features of both techniques below. After that, we briefly explain our

Manuscript received January 22, 1996; revised July 22, 1996.

The authors are with the NTT LSI Laboratories, 3-1 Morinosato Wakamiya, Atsugi, Kanagawa, 243-01, Japan.

Publisher Item Identifier S 0018-9480(96)07908-2.

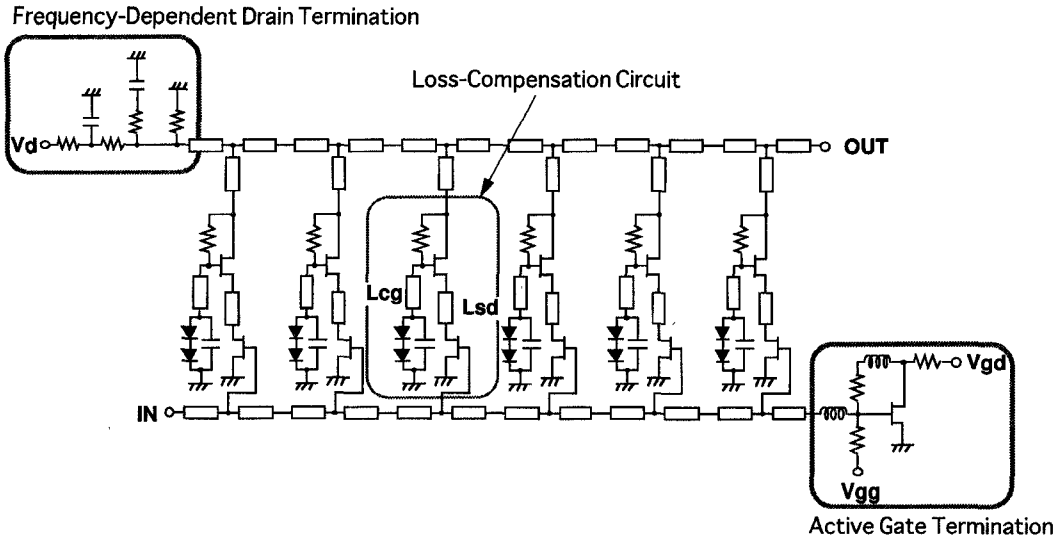

Fig. 3. Schematic circuit of the proposed distributed baseband amplifier.

loss compensation technique for improving the high-frequency performance of the amplifier.

A. *Frequency-Dependent Drain Termination*

Almost all of the distributed amplifiers reported to date do not have a flat gain response from 0 Hz. Some of them have been coupled with a capacitor as multi-stage amplifiers to achieve higher gain. Others did not have dc matching terminations to decrease their power dissipation. These amplifiers can not be used as baseband amplifiers for SDH transmission systems. Moreover, the gain of a single-stage distributed amplifier decreases at low frequencies even if it is designed with dc terminations because the output impedance of the amplifier has a frequency dependence. At high frequencies, the output impedance is almost the same as the image impedance of the artificial drain line constructed with "distributed elements;" the transmission line and parasitic capacitance of transistors. On the other hand, at low frequencies, the image impedance mainly constructed with "lumped elements;" the termination resistor and drain-to-source resistance (R_{ds}) of transistors. The output impedance at low frequencies becomes low because of the connection of the R_{ds} in parallel.

The proposed termination [Fig. 4(b)] uses a resistor-capacitor network instead of the simple resistor used in conventional termination [Fig. 4(a)]. The dc gain of a distributed amplifier is

$$A_{V(DC)} = 20 \log \frac{N \cdot g_m \cdot Z_0}{2} + 20 \log \frac{2}{2 + \dfrac{N \cdot Z_0}{R_{ds}}} \quad (1)$$

while the gain at high frequencies is

$$A_{V(RF)} = 20 \log \left| \left\{ \sum_{n=1}^{N} \frac{g_m \cdot Z_{d\pi}}{2} \cdot e^{-[(2n-1)/2]\theta_g} \cdot e^{-[(2N-2n+1)/2]\theta_d} \right\} \right|. \quad (2)$$

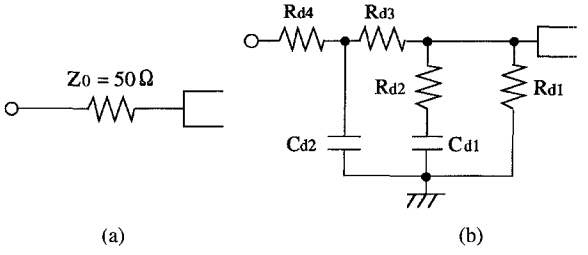

Fig. 4. Schematic circuits of the drain termination circuits of distributed amplifiers. (a) Conventional resistor termination. (b) Frequency-dependent termination.

Here, N is the number of sections in the distributed amplifier, Z_0 is the matching impedance, $Z_{d\pi}$ is the image impedance of the drain line π-section, and θ_g and θ_d are propagation functions on the drain and gate line. If $Z_{d\pi} = Z_0$, $\theta_g = \theta_d$ and attenuation constants are ignored, the gain at high frequencies equals the first term of (1). The second term of the (1) has a negative value. Therefore, the dc gain is apparently lower than the high-frequency one for the conventional design. In our work, the termination impedance increases as the frequency decreases. This compensates for the decrease of the output impedance and cancels the second term of (1).

When the termination impedance at 0 Hz is different from the matching impedance, (1) becomes

$$A_{V(DC)} = 20 \log \frac{N \cdot g_m \cdot Z_0 \cdot Z_{term}}{Z_0 + Z_{term}} + 20 \log \frac{Z_0 + Z_{term}}{Z_0 + Z_{term} + \dfrac{N \cdot Z_0 \cdot Z_{term}}{R_{ds}}}. \quad (3)$$

Here, Z_{term} is the termination impedance. The matching condition at 0 Hz is

$$Z_{term} = \frac{Z_0 \cdot R_{ds}}{R_{ds} - N \cdot Z_0} = \frac{1}{\dfrac{1}{R_{d1}} + \dfrac{1}{R_{d3} + R_{d4}}}. \quad (4)$$

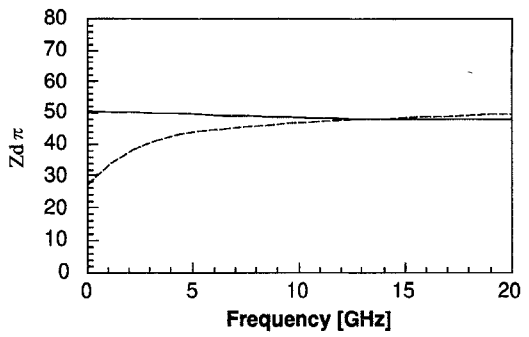

Fig. 5. Simulated image impedance of the drain line π section. Solid line: with frequency-dependent drain termination. Dotted line: with conventional resistor termination.

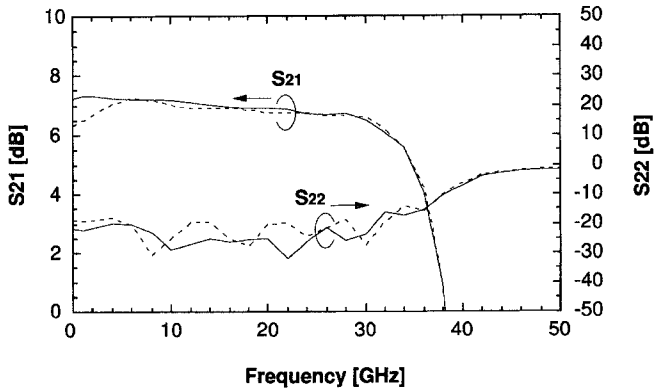

Fig. 6. Simulated S parameters of the distributed amplifiers. Solid lines: with frequency-dependent drain termination. Dotted lines: with conventional resistor termination.

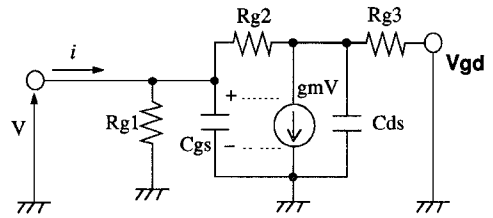

Fig. 7. Equivalent circuit of the active gate termination.

If we substitute this second term in (3), it becomes

$$A_{V(DC)} = 20 \log \frac{N \cdot g_m \cdot Z_0}{2}. \tag{5}$$

Then the gain at 0 Hz (dc gain) coincides with that at high frequencies.

The simulated image impedance of the drain line (this is the average value of $Z_{d\pi}$ of all sections) and S parameters are shown in Figs. 5 and 6, respectively. A very flat $Z_{d\pi}$, a very flat S_{21}, and lower S_{22} are achieved from 0 Hz compared with conventional resistor termination.

B. Active Gate Termination

This termination uses FET with a feedback resistor. The noise figure of a distributed amplifier is degraded due to the gate termination's noise contribution at low frequencies [6]. The new circuit makes the thermal noise voltage lower than with the simple resistor termination at low frequencies because it uses a feedback-matching scheme. Fig. 7 shows the equivalent circuit of the termination circuit. In this figure, we don't show R_d, R_g, R_s, R_i, and C_{dg}. If we use a resistor with a large value for R_{g1}, the matching condition is approximately expressed as

$$\begin{aligned} Z_0 &= \frac{V}{i} \\ &\approx \frac{R_{g2} + R_{g3}}{1 + g_m R_{g3}} \\ &\approx \frac{\dfrac{R_{g2}}{R_{g3}} + 1}{g_m}. \end{aligned} \tag{6}$$

Fig. 8 shows the equivalent circuit with the thermal noise voltage sources of the resistors, e_{n2} and e_{n3}, and drain noise current source, i_D. The thermal noise voltage of this termination is

$$\begin{aligned} \sqrt{\overline{|E_n|^2}} &= \sqrt{\overline{|e_{n2}|^2}} + \sqrt{\overline{|e_{n3}|^2}} \\ &\quad + R_{g3}\left(\sqrt{\overline{|i_D|^2}} - g_m\sqrt{\overline{|E_n|^2}}\right) \\ \overline{|e_{n2}|^2} &= 4kT \cdot R_{g2} \cdot \Delta f \\ \overline{|e_{n3}|^2} &= 4kT \cdot R_{g3} \cdot \Delta f. \end{aligned} \tag{7}$$

Therefore, the noise spectral density becomes

$$\frac{\overline{|E_n|^2}}{\Delta f} = 4kT \frac{R_{g2} + R_{g3} + g_m R_{g3}^2 \cdot P}{(1 + g_m R_{g3})^2} \tag{8}$$

where P is the drain noise coefficient defined as

$$P \equiv \frac{\overline{|i_D|^2}}{4kT \cdot \Delta f \cdot g_m}. \tag{9}$$

When we substitute the matching condition (6) in (8), the noise spectral density is approximately given as

$$\begin{aligned} \frac{\overline{|En|^2}}{\Delta f} &\approx 4kT\left[\frac{Z_0}{1 + g_m R_{g3}} + \frac{g_m R_{g3}^2 \cdot P}{(1 + g_m R_{g3})^2}\right] \\ &\approx 4kT\left(\frac{Z_0}{g_m \cdot R_{g3}} + \frac{P}{g_m}\right). \end{aligned} \tag{10}$$

It is clear that we can make the spectral density lower than that of conventional resistor termination ($= 4kTZ_0$) when we use a high-g_m transistor (a wide gate-width transistor). However, the large input capacitance, C_{gs}, of the transistor degrades the high-frequency performance of the amplifier. For this reason, we used spiral inductors as shown in Fig. 3 to keep the matching condition up to millimeter wave frequencies.

The simulated noise figure and gain are compared in Fig. 9. In the simulation, the gate-termination impedance was fixed at 50 Ω. And the effects of $1/f$ (flicker) noise and generation-recombination noise were not included. One can see that the noise figure improved without any degradation of gain performance.

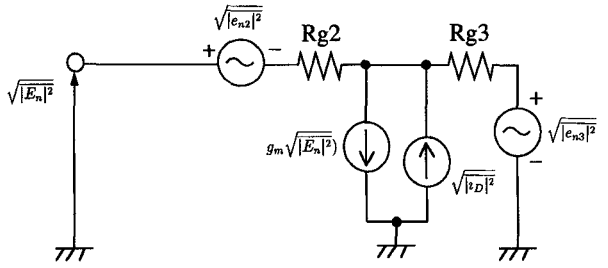

Fig. 8. Equivalent circuit of the active gate termination with noise voltage and current sources.

C. Loss-Compensation Technique

The distributed amplifier has been used for broadband applications, but can not achieve the essential wide band characteristics due to the losses of gate and drain lines. Recently, the cascode pair of transistors have been used for the distributed amplifiers to obtain wide band characteristics because the common-gate transistor of the cascode transistors provides a broadband loss compensation for the drain line [7]. The output impedance of the cascode pair is

$$Z_{out} = \frac{Z_{ds1}}{Z_{ds1} + Z_{gs2}} \left(\frac{g_m \cdot Z_{ds2}}{j\omega C_{gs2}} + Z_{gs2} \right) + Z_{ds2} \qquad (11)$$

where Z_{gs} and Z_{ds} are the gate-to-source and drain-to-source impedance of a transistor, respectively and 1 and 2 indicate a common-source and common-gate transistor. The first term on the right in the (11) operates as a negative resistance and compensate the losses of the drain artificial line. However, this negative resistance effect cannot be controlled by circuit design techniques because it depends only on the parameters of the transistors. And if we use transistors whose C_{gs} and C_{ds} values are close, the high gate-source impedance Z_{gs2} weakens the loss compensation effect in the millimeter-wave frequency region.

This led us to develop a new loss compensation technique [5]. The schematic diagram of the loss-compensated distributed amplifier is shown in Fig. 3. It has additional transmission lines at the gate terminal of the common-gate FET (L_{cg}) and one between two FET's (L_{sd}). Therefore, the output impedance can be written by

$$Z_{out} = \frac{Z_{ds1} + j\omega L_{sd}}{(Z_{ds1} + j\omega L_{sd}) + (Z_{gs2} + j\omega L_{cg})} \times \left[\frac{g_m \cdot Z_{ds2}}{j\omega C_{gs2}} + (Z_{gs2} + j\omega L_{cg}) \right] + Z_{ds2}. \qquad (12)$$

L_{cg} decreases Z_{gs2} in the first fraction's denominator. Therefore, the negative resistance increases and the S_{21} of the amplifier is improved in the high-frequency region. However, the stability of the amplifier is lost when the real part of the output impedance $\mathrm{Re}\,(Z_{out})$ becomes negative. The addition of L_{sd} decreases Z_{ds1} in the fraction. It softens the effect of L_{cg} and restores stability. Fig. 10 clearly shows the effect. Simulated S_{21} and S_{22} are superior at high frequencies and simulated GBWP increases 22% over that of an optimized conventional cascode distributed amplifier.

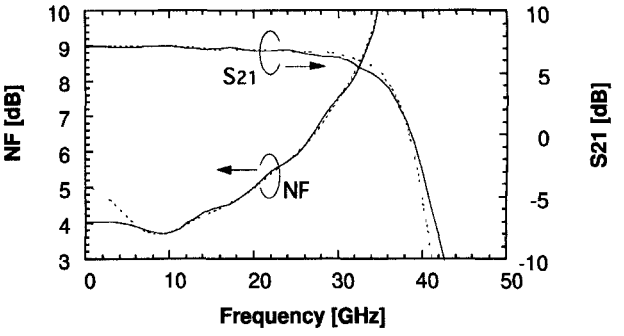

Fig. 9. Simulated noise figure and gain of the distributed amplifiers. Solid lines: with active gate termination. Dotted lines: with conventional resistor termination.

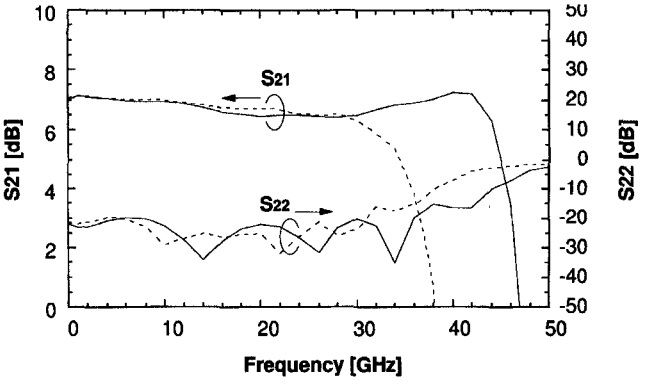

Fig. 10. Simulated S parameters of the distributed baseband amplifier. Solid lines: with loss compensation circuit. Dotted lines: with conventional cascode pair of transistors.

III. Fabrication

The amplifier IC's were fabricated using 0.2-μm gate-length GaAs MESFET's [8] by NTT Electronics Technology Corporation. f_T and $f_{\max}$ were 40 and 80 GHz. Coplanar waveguide technology was used for the transmission lines. We made two kinds of IC's: One with active gate termination and frequency-dependent drain termination with a conventional derived m-type filter configuration [Fig. 11(a)] and another with loss compensation circuits and frequency-dependent drain termination [Fig. 11(b)]. We call them the "low-noise type" and "loss-compensated type." Microphotographs of these amplifiers are shown in Fig. 12. Both of the chips are 1.5×2.5 mm.

IV. Circuit Performance

A. S Parameters

The amplifier IC's were measured on wafers using RF probes and a network analyzer. Measured S parameters of the amplifier IC's are shown in Fig. 13. Both IC's have a gain of 9 dB (higher than the simulated data in Figs. 6, 9, and 10 by 2 dB). They also have a flat gain from 0 Hz without any off-chip components because of the frequency-dependent drain terminations. The gain of the loss-compensated-type amplifier IC [Fig. 13(b)] was improved compared with that of the low-noise-type (conventional) one [Fig. 13(a)] at high frequencies. The low-noise-type and loss-compensated-type

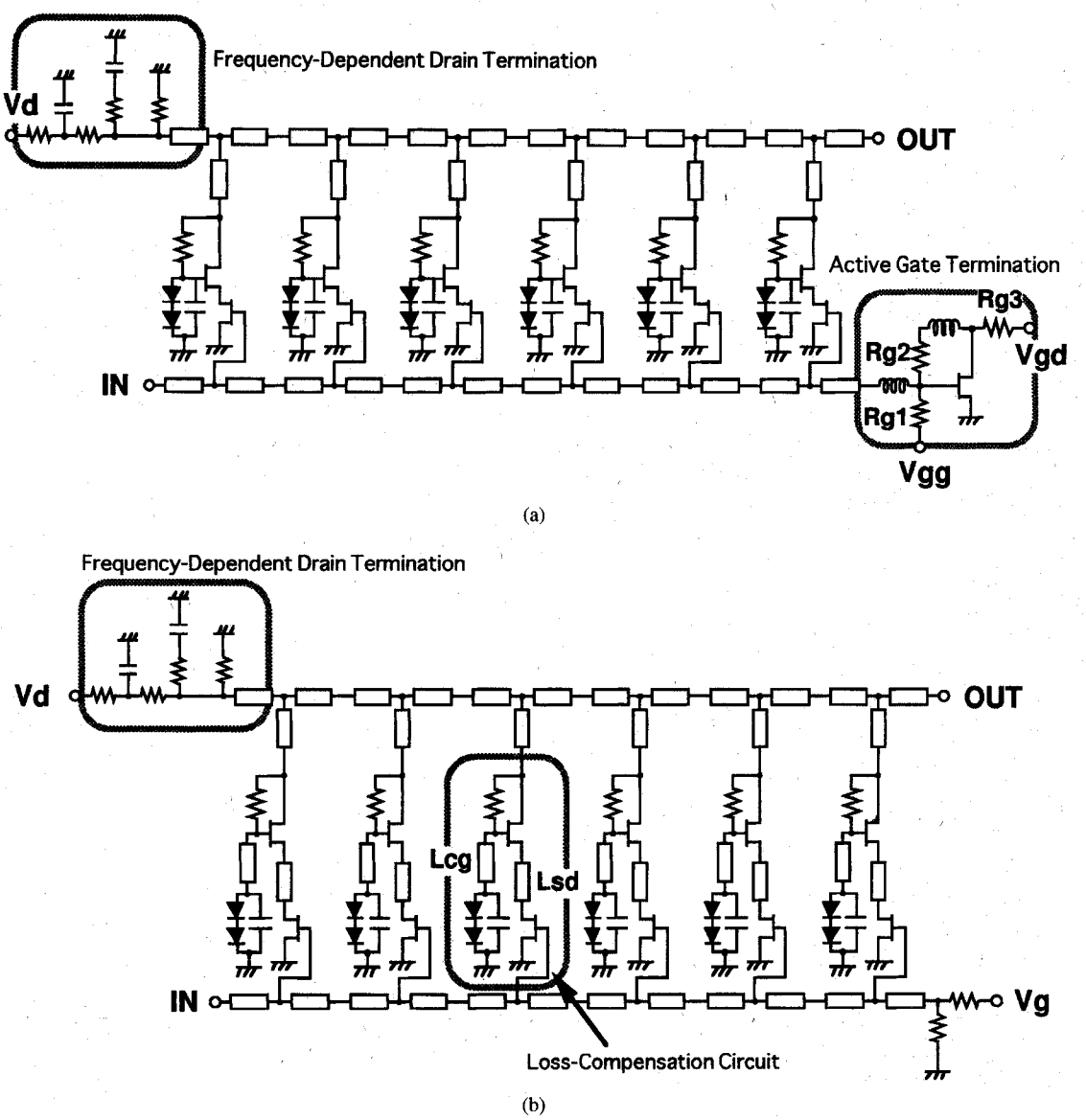

Fig. 11. Schematic circuits of the distributed baseband amplifier IC's. (a) Low-noise-type amplifier IC. (b) Loss-compensated-type amplifier IC.

amplifier IC's have 3-dB bandwidths of 36 and 44 GHz, and power dissipation of 1.2 and 1.0 W, respectively. S_{11} and S_{22} of the low-noise-type amplifier IC are less than -12.2 and -16.5 dB below 36 GHz. Those of the loss-compensated-type amplifier IC are less than -16.9 and -9.7 dB below 40 GHz, and less than -9.8 dB (at 44 GHz) and -6.5 (at 44 GHz) below 44 GHz. The measured group delays of S_{21} are shown in Fig. 14. The delay of the low-noise-type and the loss-compensated-type amplifier IC's are about 60 and 50 ps below 28 GHz (an upper limit frequency of at least 28 GHz is required for 40-Gb/s optical transmission). These results show that the loss compensation circuit also improves the flatness of the group delay characteristics at high frequencies.

B. Noise Figures

The effect of the active gate termination is shown in Fig. 15. The measurement was again done on wafers using RF probes and a noise figure meter. Measured NF of the low noise-type amplifier IC was improved 0.7 dB compared with the resistor termination of the loss-compensated-type amplifier IC below 7 GHz while keeping return loss low. The average NF of the low-noise-type and loss-compensated-type amplifier IC's are 4.2 and 4.9 dB below 7 GHz, respectively. The measured noise figure at higher frequencies is shown in Fig. 16. The average NF of the low-noise-type amplifier IC is 5.4 dB below 36 GHz and that of the loss-compensated-type amplifier IC is 5.4 dB below 40 GHz, respectively.

V. Conclusion

Advanced design techniques and the performance of a GaAs MESFET distributed amplifier built with these techniques were described. A key feature of the design is the use of a frequency-dependent drain termination and active gate termination to achieve a 0-Hz-to-millimeter-wave bandwidth with a low noise figure. The amplifier IC has a flat gain of 9 dB with a 0–36-GHz bandwidth. And the low-noise circuit scheme showed a noise figure of 4 dB, about 1 dB lower than the conventional distributed amplifier at low frequencies. Another amplifier IC,

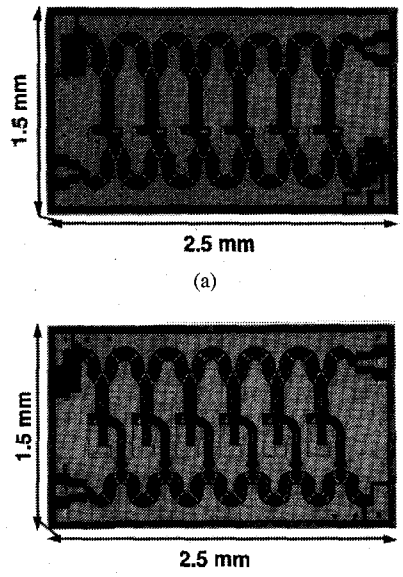

Fig. 12. Microphotographs of the distributed baseband amplifier IC's. (a) Low-noise-type amplifier IC. (b) Loss-compensated-type amplifier IC.

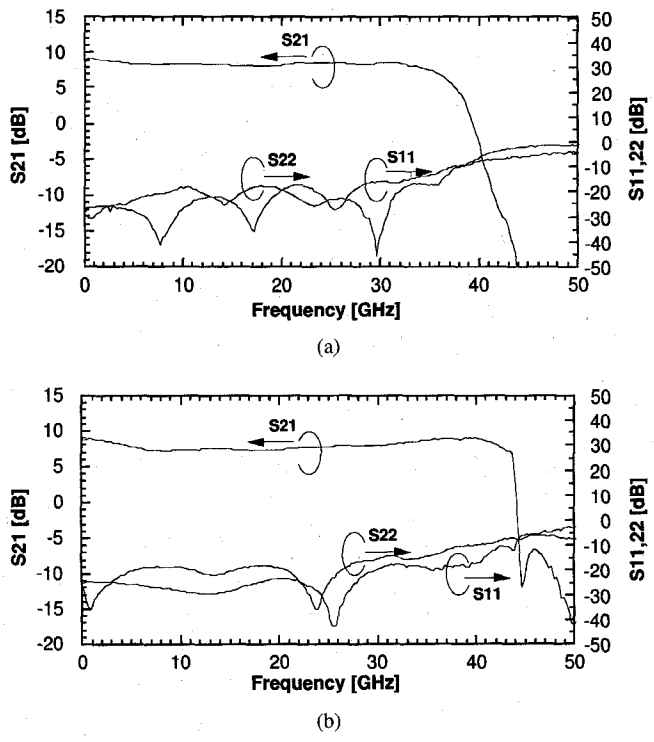

Fig. 13. Measured S parameters of the distributed baseband amplifier IC's. (a) Low-noise-type amplifier IC. (b) Loss-compensated-type amplifier IC.

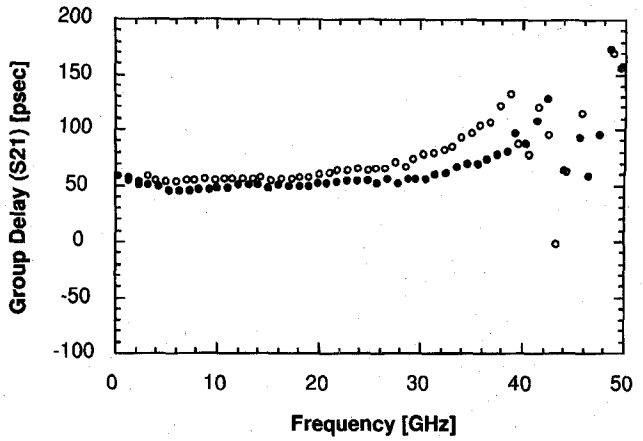

Fig. 14. Measured group delay of the distributed baseband amplifier IC's. Open circles: low-noise-type amplifier IC. Closed circles: loss-compensated-type amplifier IC.

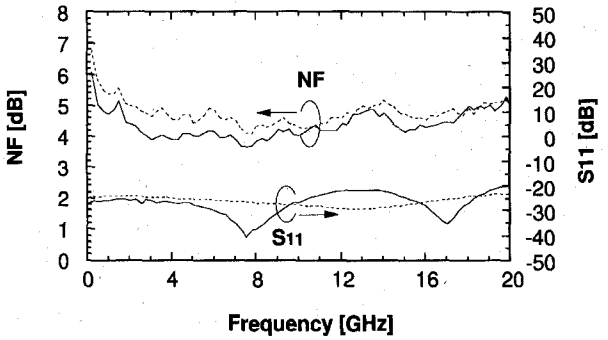

Fig. 15. Measured noise figure and S_{11} of the distributed baseband amplifier IC's below 20 GHz. Solid lines: low-noise-type amplifier IC. Dotted lines: loss-compensated-type amplifier IC.

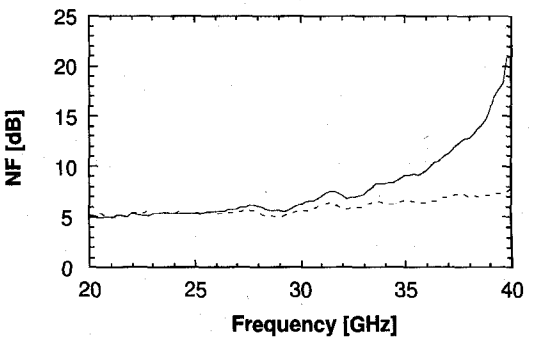

Fig. 16. Measured noise figure of the distributed baseband amplifier IC's over 20 GHz. Solid line: low-noise-type amplifier IC. Dotted line: loss-compensated-type amplifier IC.

built using our loss compensation circuit, also has a flat gain of 9 dB with a 0–44-GHz bandwidth. To our knowledge, this is the widest bandwidth ever reported for state-of-the-art baseband amplifier IC's using commercially-available GaAs MESFET's. These results will have considerable impact on the development of 40-Gb/s optical communication systems.

ACKNOWLEDGMENT

The authors would like to thank Dr. S. Horiguchi, E. Sano, and Dr. T. Shibata for their encouragement and suggestions throughout this work. We also thank K. Hagimoto and Y. Miyamoto for their giving opportunity of device fabrication.

REFERENCES

[1] Y. Imai, E. Sano, and K. Asai, "Design and performance of wideband GaAs MMIC's for high-speed optical communication systems," *IEEE Trans. Microwave Theory Tech.*, vol. 40, pp. 185–190, Feb. 1992.

[2] Y. Ayasli, S. W. Miller, R. Mozzi, and L. K. Hanes, "Capacitively coupled traveling-wave power amplifier," *IEEE Trans. Microwave Theory Tech.*, vol. 32, pp. 1704–1709, Dec. 1984.

[3] R. Majidi-Ahy, C. K. Nishimoto, M. Riaziat, M. Glenn, S. Silverman, S. Weng, Y. Pao, G. A. Zdasiuk, S. G. Bandy, and Z. C. H. Tan, "5–100

GHz InP coplanar waveguide MMIC distributed amplifier," *IEEE Trans. Microwave Theory Tech.*, vol. 38, pp. 1986–1993, Dec. 1990.
[4] J. Pusl, B. Agarwal, R. Pullela, L. D. Nguyen, M. V. Le, M. J. W. Rodwell, L. Larson, J. F. Jensen, R. Y. Yu, and M. G. Case, "Capacitive-division traveling-wave amplifier with 340 GHz gain-bandwidth product," in *1995 MMWMC Dig.*, May 1995, pp. 175–178.
[5] S. Kimura, Y. Imai, Y. Umeda, and T. Enoki, "A 16-dB DC-50 GHz InAlAs/InGaAs HEMT distributed baseband amplifier using a new loss compensation technique," in *1994 GaAs IC Symp. Dig.*, Oct. 1994, pp. 96–99.
[6] K. B. Niclas and R. R. Pereira, "Performance of a 2–18 GHz ultra low-noise amplifier module," in *IEEE MTT-S Int. Microwave Symp. Dig.*, June 1989, vol. CC-1, pp. 841–844.
[7] S. Deibele and J. B. Beyer, "Attenuation compensation in distributed amplifier design," *IEEE Trans. Microwave Theory Tech.*, vol. 37, pp. 1425–1433, Sept. 1989.
[8] Y. Yamane, M. Ohhata, H. Kikuchi, K. Asai, and Y. Imai, "A 0.2 μm GaAs MESFET technology for 10 Gb/s digital and analog IC's," in *IEEE MTT-S Int. Microwave Symp. Dig.*, June 1991, vol. Q-1, pp. 513–516.

Shunji Kimura (M'92) was born in Tokyo, Japan, on January 28, 1967. He received the B.S. and M.S. degrees in electrical engineering from Waseda University, Tokyo, Japan, in 1989 and 1991, respectively.

In 1991, he joined Nippon Telegraph and Telephone Corporation (NTT) LSI Laboratories, Kanagawa, Japan. He has been engaged in design and evaluation of microwave and millimeter-wave monolithic integrated circuits for optical transmission systems.

Mr. Kimura received the Japan Microwave Prize at the 1994 Asia-Pacific Microwave Conference. He is a member of the Institute of Electronics, Information, and Communication Engineers (IEICE) of Japan and the Physical Society of Japan.

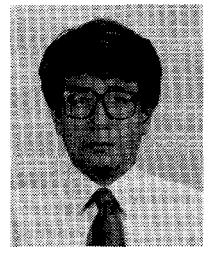

Yuhki Imai (M'92) was born in Tokyo, Japan, in 1955. He received the B.S., M.E., and Dr.Eng. degrees in applied physics from Waseda University, Tokyo, Japan, in 1977, 1979, and 1991, respectively.

In 1979, he joined the NTT Electrical Communication Laboratories. He has been engaged in the research of microwave GaAs and InP MESFET fabrication technologies, low-current GaAs MMIC design for mobile communications and high-speed GaAs IC design for 10-Gb/s lightwave communications. He is now engaged in the research of future very high-speed IC design using GaAs and InP-based devices.

Dr. Imai received the Japan Microwave Prize at the 1994 Asia-Pacific Microwave Conference. He is a member of the Institute of Electronics, Information, and Communication Engineers (IEICE) of Japan.